

Modulation of catalyst enantioselectivity through reversible assembly of supramolecular helices.

Yan Li, Xavier Caumes, Matthieu Raynal* and Laurent Bouteiller

Supporting Information

General Procedures.	3
Evaluation of salts and solvents in catalysis (Table S1)	6
Characterization of the “pristine” co-assemblies (Figs. 2, S1-S3).	7
Characterization of the “pristine” co-assemblies coordinated to Cu (Fig. S4).	11
Characterization of the co-assemblies in presence of additives at concentrations <i>ca.</i> 4 times lower than those of catalytic experiments (Figs. S5-S6).	13
Characterization of the co-assemblies in presence of additives at concentrations close to those of catalytic experiments (Figs. 2, S7-S8).	16
Summary of the structural data and correlation between length and selectivity (Table S2). ...	19
Reversible switch of the selectivity (Table S3).	20
Catalytic experiments.	21
GC analyses from the aliquots of the different run.	22
References.	25

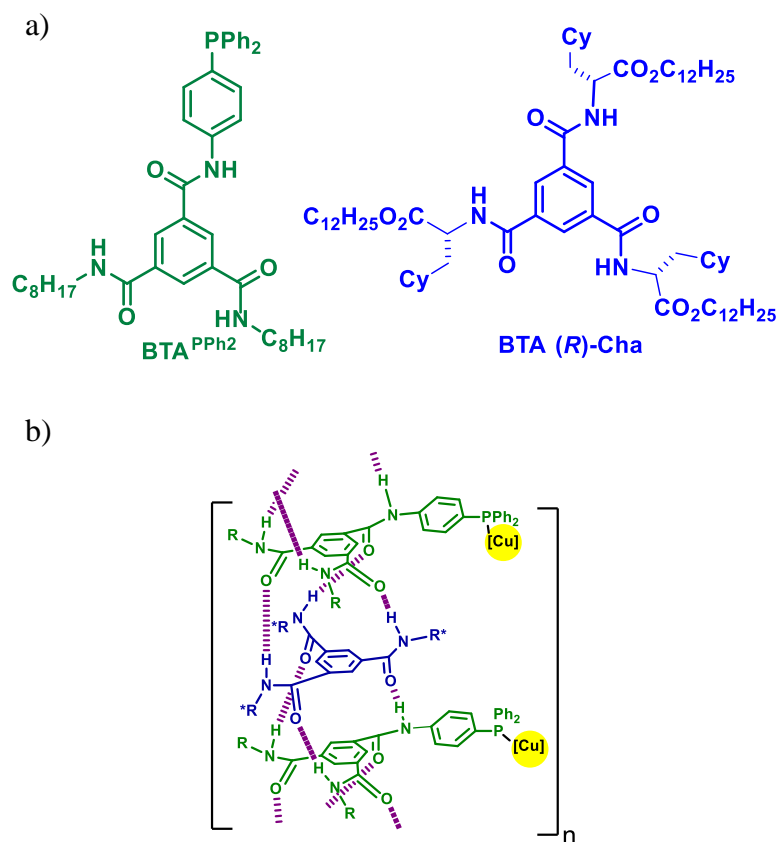


Chart S1 a) Chemical structures of the BTA molecules investigated in this study. b) Representation of the rod-like co-assemblies between **BTA^{PPh₂}** and **BTA (R)-Cha**. The ratio ligand: co-monomer ($\approx 2:1$) reflects the composition determined by analytical techniques (see below). It provides predominantly the (*S*) product in the hydrosilylation of the 1-(4-nitrophenyl)ethanone.¹ (The distribution of the two BTAs along the rod is not known as well as the coordination mode and the fraction of coordinated PPh₂ groups in the co-assemblies).

General Procedures.

BTA^{PPh₂},¹ and **BTA (R)-Cha**,² were prepared according to published procedures. PhSiH₃ (>97%, Sigma-Aldrich), Cu(OAc)₂·H₂O (>99%, Sigma-Aldrich), 1-(4-nitrophenyl)ethanone (NPhone, >98% Alfa Aesar), TBANTf₂ (purity ≥ 99%, Fluka) and NaNTf₂ (purity ≥ 98%, Fluorochem) were stored under vacuum prior to use. Dried solvents were obtained from an SPS solvent purification system (IT-Inc).

Fourier-Transform Infrared (FT-IR) analyses: FT-IR measurements were performed on a Nicolet iS10 spectrometer. Spectra were measured in 0.02 cm pathlength CaF₂ cells at 293 K and were corrected for air, solvent and cell absorption.

Deconvolution procedure for quantitative analysis of FT-IR spectra - determination of f Cha in stacks and DP_n (Figs. S2 and S7): The bands corresponding to ester C=O (1717-1753 cm⁻¹) and amide C=O (1627-1680 cm⁻¹) in the FT-IR spectra of different samples (**BTA (R)-Cha**, **BTA^{PPh₂}**, co-assemblies with and without salts) are deconvoluted simultaneously into two Gaussian peaks and three Gaussian peaks respectively. The procedure yields five bands with the same position and width for each sample but with different intensities: free ester (≈1745 cm⁻¹), bonded ester (≈1725 cm⁻¹), free amide (≈1671 cm⁻¹), bonded amide peak 1 (≈1650 cm⁻¹) and bonded amide peak 2 (≈1635 cm⁻¹). The molar extinction coefficients of the bonded amide peak 2, the free amide peak and the bonded ester peak were obtained from the individual spectra of **BTA^{PPh₂}** and **BTA (R)-Cha**. Then, the fraction of **BTA (R)-Cha** in stacks (f Cha in stacks) and the DP_n values are obtained by means of the following formula:

$$[\text{BTA Cha dimers}] = \frac{\text{area of bonded ester band}}{\epsilon_{\text{bonded ester}} \times \text{pathlength}}$$

$$[\text{BTA Cha in stacks}] = [\text{BTA Cha}]_0 - [\text{BTA Cha dimers}]$$

$$\mathbf{f \text{ Cha in stacks}} = \frac{[\text{BTA Cha in stacks}]}{[\text{BTA}^{\text{PPh}_2}]_0 + [\text{BTA Cha in stacks}]}$$

$$[\text{bonded amide functions}] = \frac{\text{area of bonded amide bands 1 and 2}}{\epsilon_{\text{bonded amide}} \times \text{pathlength}}$$

$$[\text{free amide functions}] = \frac{\text{area of free amide band}}{\epsilon_{\text{free amide}} \times \text{pathlength}}$$

$$[\text{stack end}] = [\text{free amide functions}] - [\text{BTA Cha dimers}]$$

$$\mathbf{DP_n} = 1 + \frac{[\text{bonded amide functions}]}{[\text{stack end}]}$$

with [BTA Cha]₀ and [BTA^{PPh₂}]₀ the introduced amount of the respective monomers in the mixture. $\epsilon_{\text{bonded ester}}$, $\epsilon_{\text{bonded amide}}$ and $\epsilon_{\text{free amide}}$ are the molar extinction coefficients of the corresponding functions. Low values for [stack end] (and thus large values for DP_n) cannot be reliably determined by this approach.

Circular dichroism (CD) analyses: CD measurements were performed on a Jasco J-1500 spectrometer equipped with a Peltier thermostated cell holder and Xe laser. Data were recorded at 20°C with the following parameters: 20 nm.min⁻¹ sweep rate, 0.05 nm data pitch, 2.0 nm bandwidth, and between 400 and 270 nm. Toluene and cell contributions at the same temperature were subtracted from the obtained signals. A dismountable quartz cell of 0.01 mm pathlength was used. For all samples, LD contribution was negligible ($\Delta LD < 0.005$ dOD) and the shape of the CD signal was independent of the orientation of the quartz slide. Molar CD values are reported in L.mol⁻¹.cm⁻¹ and are expressed as follows: $\Delta\epsilon = \theta / (32980 \times l \times c)$ where θ is the measured ellipticity (mdeg), l is the optical path length in cm, and c is the concentration in mol.L⁻¹.

Small-angle neutron scattering (SANS) analyses: SANS measurements were made at the LLB (Saclay, France) on the PA20 instrument, at three distance-wavelength combinations to cover the 2.4×10^{-3} to 0.46 \AA^{-1} q -range, where the scattering vector q is defined as usual, assuming elastic scattering, as $q = (4\pi/\lambda)\sin(\theta/2)$, where θ is the angle between incident and scattered beam. Data were corrected for the empty cell signal and the solute and solvent incoherent background. A light water standard was used to normalize the scattered intensities to cm⁻¹ units. The data was fitted with the DANSE software SasView. The number n of molecule in the cross-section can be derived from n_L (the number of molecule per unit length)³ by assuming an average intermolecular distance of 3.62 Å, which is the usual spacing between aromatic rings in BTA helical assemblies.

Preparation of BTA solutions for CD (Fig. 2b), NMR (Figs. S3 and S8) and FT-IR (Figs. 2a, S7 and S2) analyses of the co-assemblies without Cu: The concentrations are close to those employed in the catalytic experiments. A stock solution (6.0 mL) was prepared by dissolving **BTA^{PPh2}** (16.7 mM) and **BTA (R)-Cha** (18.4 mM) in C₇D₈. The vial was sealed with a PTFE-coated cap to avoid contamination from leaching plasticizer, gently heated for ensuring dissolution and placed on a shaking table for 12 h. Four samples were prepared from the same stock solution:

- “pristine” co-assemblies: a given amount of this stock solution was directly used for analyses (298 K).
- co-assemblies + TPPCl: TPPCl (1.0 equiv. relatively to **BTA^{PPh2}**) dissolved in CD₂Cl₂ (40 μL) was added to an aliquot (600 μL) of this stock solution, the solution was stirred for 1 hour, and a given amount was taken for analyses.
- co-assemblies + TPPCl + NaNTf₂: TPPCl (1.0 equiv.) dissolved in CD₂Cl₂ (40 μL) and NaNTf₂ (1.0 equiv.) dissolved in acetone-d₆ (40 μL) were added to an aliquot (600 μL) of the stock solution, the solution was stirred for 1 hour, and a given amount was taken for analyses.
- co-assemblies + DCM + acetone: CD₂Cl₂ (40 μL) and acetone-d₆ (40 μL) were added to an aliquot (600 μL) of the stock solution, the solution was stirred for 1 hour, and a given amount was taken for analyses.

All samples were heated prior to analysis

Preparation of BTA solutions for NMR (Fig. S4a) and FT-IR (Fig. S4b) analyses of the co-assemblies with Cu: The concentrations are close to those employed in the catalytic experiments. Sample “pristine co-assemblies·Cu”: A stock solution (3.0 mL) was prepared by dissolving **BTA^{PPh2}** (16.7 mM), Cu(OAc)₂·H₂O (8.35 mM), and **BTA (R)-Cha** (18.4 mM) in THF and stirring for 12 h. The THF was removed under vacuum

and the obtained solid was dried for 1 h. C₇D₈ (3.0 mL) was added and the mixture was stirred for 12 h. The sample was heated prior to analysis.

Preparation of BTA solutions for SANS analyses - characterization of the co-assemblies (Fig. S1): Three samples were prepared by dissolving **BTA**^{PPh₂} (5.98 g.L⁻¹, 8.6 mM), **BTA (R)-Cha** (19.9 g.L⁻¹, 16.9 mM), and a mixture of **BTA**^{PPh₂} (3.98 g.L⁻¹, 5.8 mM) and **BTA (R)-Cha** (4.39 g.L⁻¹, 3.7 mM) in C₇D₈.

Preparation of BTA solutions for SANS analyses - addition of salts (Fig. S5): A stock solution A was prepared by dissolving **BTA**^{PPh₂} (41.0 mg) and **BTA (R)-Cha** (45.0 mg) in 4.088 g of THF. A stock solution B was obtained by dissolving CuOAc·H₂O (3.95 mg) in 2.698 g of stock solution A. Three samples were prepared from stock solution B:

- **SANS co-assemblies·Cu:** 399.8 mg of stock solution B was taken, the solvent was removed under vacuum and the tube was further put under vacuum (1.10⁻³ mbar) for 1 hour. 939.7 mg of C₇D₈ was added and the vial was sealed with PTFE-coated cap and placed on a shaking table for 12 h
- **SANS co-assemblies·Cu + TPPCl:** 1.097 g of stock solution B was added to a vial containing TPPCl (7.10 mg). The mixture was stirred for 1 h, the solvent was removed under vacuum and the tube was further put under vacuum (1.10⁻³ mbar) for 1 hour. 2.600 g of C₇D₈ was added and the vial was sealed with PTFE-coated cap, gently heated to ensure dissolution and placed on a shaking table for 12 h
- **SANS co-assemblies·Cu + TPPCl + NaNTf₂:** 1.097 g of stock solution B was added to a vial containing TPPCl (7.03 mg) and NaNTf₂ (4.73 mg). The mixture was stirred for 1 h, the solvent was removed under vacuum and the tube was further put under vacuum (1.10⁻³ mbar) for 1 hour. 2.596 g of C₇D₈ was added and the vial was sealed with PTFE-coated cap, gently heated to ensure dissolution and placed on a shaking table for 12 h.

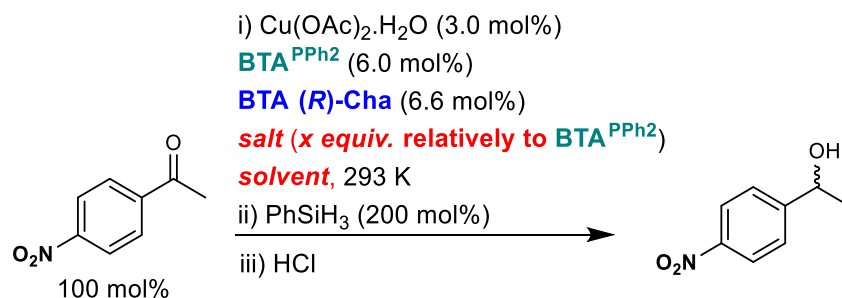
All samples have been heated prior to analysis. The concentrations of the different components for the three samples are indicated in Fig. S5. These samples have also been analysed by FT-IR (Fig. S6).

Chiral GC analyses: 1-(4-nitrophenyl)ethanol (NPnol). The optical purity was determined by GC analysis: Chiral Cyclosil-B column, 30 m × 250 μm × 0.25 μm, inlet pressure = 12.6 psi. Injection temperature = 250°C; detector temperature = 300°C; column temperature = 145°C. Retention time: 17.9 min (1-(4-nitrophenyl)ethanone), 47.6 min ((R)-enantiomer), 49.9 min ((S)-enantiomer).⁴

Catalytic experiments: see detailed procedures in page S-21.

Evaluation of salts and solvents in catalysis (Table S1)

Table S1 Influence of solvent, concentration and salts on the selectivity of the catalytic co-assemblies for the copper-catalysed hydrosilylation of 1-(4-nitrophenyl)ethanone (NPnone).



entry	solvent	[NPnone]	salt/equivalent	conversion (%, after 1h)	selectivity (<i>e.e.</i>)
1	toluene	0.28 M	-	>99	54±1 ¹
2	THF	0.28 M	-	>99	0
3	toluene	0.008 M ^[a]	-	<i>nd</i>	19
4	toluene:DCM 15:1	0.26 M	TPPCI/0.3	>99	44
5	toluene:DCM 15:1	0.26 M	TPPCI/0.5	97	40
6	toluene:DCM 15:1	0.26 M	TPPCI/0.75	91	23
7	toluene:DCM 15:1	0.26 M	TPPCI/0.85	75	8
8	toluene:DCM 15:1	0.26 M	TPPCI/1.0	63	0
9	toluene	0.28 M	$\text{NaCl}/1.0$	>99	53
10	toluene	0.28 M	$\text{TBANTf}_2/1.0$ ^[b]	>99	51

Reaction conditions: 1-(4-nitrophenyl)ethanone (NPnone), $\text{Cu}(\text{OAc})_2 \cdot \text{H}_2\text{O}$ (3.0 mol%), $\text{BTA}^{\text{PPh}_2}$ (6.0 mol%), BTA (R)-Cha (6.6 mol%), PhSiH_3 (200 mol%), solvent, 293 K, 12 h. Conversion > 90% as determined by GC analyses. The *e.es.* were determined by chiral GC analyses⁴ and are given with an error bar of ±1.5% except for entry 1 ±1%.¹ For reactions with TPPCI: TPPCI is introduced in DCM such as the solvent mixture for the catalytic experiment is toluene:DCM 15:1. Nd : not determined.

[a] $[\text{BTA}^{\text{PPh}_2}] = 0.5 \text{ mM}$ which is close to the critical concentration for self-assembly.¹

[b] TBANTf_2 and TPPNTf_2 (the latter being the salt generated upon the salt metathesis reaction) are expected to behave similarly.

Characterization of the “pristine” co-assemblies (Figs. 2, S1-S3).

The length of the co-assemblies at a concentration of $[\text{BTA}^{\text{PPh}_2}] = 5.8 \text{ mM}$ and $[\text{BTA (R)-Cha}] = 3.7 \text{ mM}$ is determined to be 870 \AA , *i.e.* $\text{DP}_n = 125$ by SANS (Fig. S1). For the catalytic experiments, the concentrations are *ca.* 4 times higher ($[\text{BTA}^{\text{PPh}_2}] = 16.7 \text{ mM}$ and $[\text{BTA (R)-Cha}] = 18.3 \text{ mM}$), so that a value twice higher is expected ($\text{DP}_n \approx 250$).⁵ FT-IR measurements (Fig. S2) are in agreement with this order of magnitude because the concentration of stack ends is too low to be determined. These analyses also allow to determine a fraction of **BTA (R)-Cha** in stacks equals to 0.33. The co-assembly process from monomers (378 K) to stacks (293 K) is probed by NMR (Fig. S3). Finally, CD analysis of the co-assembly is consistent with the formation of homochiral left-handed helices (Fig. 2b).

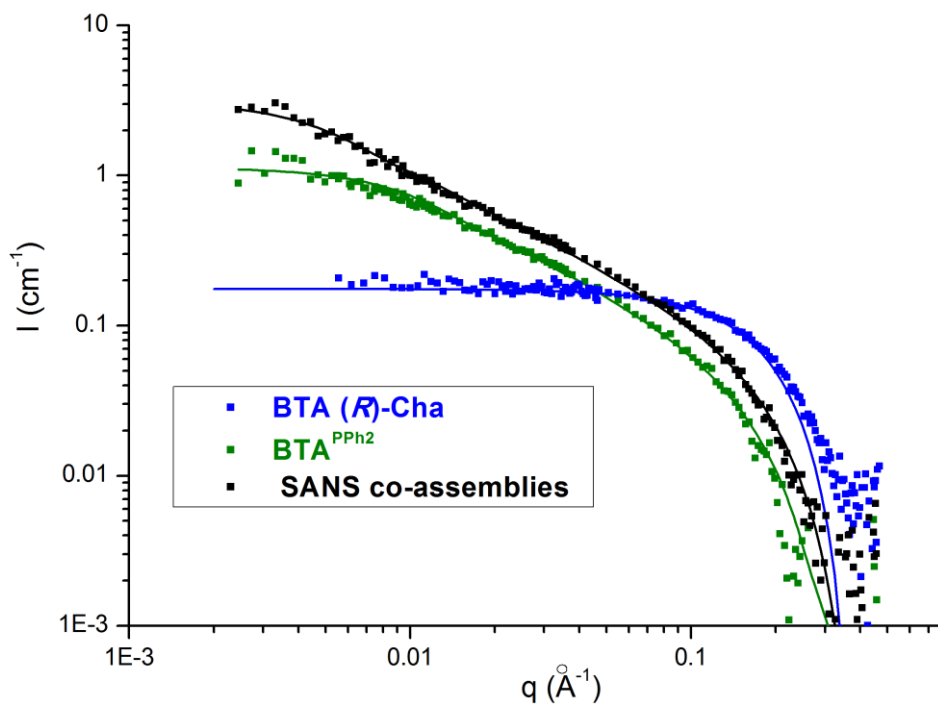


Figure S1 Characterization of the co-assemblies by SANS analyses (293 K, C₇D₈).^{[a],[b],[c]}

[a] Composition and result of the fits (n: number of molecule in the cross-section):

sample	[BTA (<i>R</i>)-Cha]	[BTA ^{PPh2}]	r (Å) ^[b]	n	length(Å)/ DP _w ^[b]	f Cha in stacks ^[b]
BTA (<i>R</i>)-Cha	19.9 g.L ⁻¹ 16.9 mM	-	12.0	-	dimer	-
BTA^{PPh2}		5.98 g.L ⁻¹ 8.6 mM	11.1	0.7	420/120	-
SANS co-assemblies	4.39 g.L ⁻¹ 3.7 mM	3.98 g.L ⁻¹ 5.8 mM	10.4	0.6	870/250	0.33

[b] SANS data of **BTA (*R*)-Cha** is fitted according to the form factor for spherical objects. The molar mass of the spherical object ($M=1993$ g/mol) is 1.7 times the molar mass of the monomer which is consistent with **BTA (*R*)-Cha** being a dimer. This dimer was thoroughly characterized in our previous reports.^{2, 6, 7}

SANS data of **BTA^{PPh2}** is fitted according to the form factor for rigid rods of finite length with a circular cross-section and a uniform scattering length density. It gives a radius of 11.1 Å, a number of molecules in the cross-section $n=0.7$ (which is consistent with isolated stacks of BTAs) and a length of 420 Å ($DP_w \approx 120$).

It was previously shown that **BTA (*R*)-Cha** in part co-assembles with **BTA^{PPh2}** and that the remaining **BTA (*R*)-Cha** exists as dimers.¹ Therefore, SANS data of the mixture of **BTA^{PPh2}** and **BTA (*R*)-Cha** is fitted as the sum of the form factors for spherical objects and for rigid rods of finite length. The latter yields a length of 870 Å ($DP_w \approx 250$, $DP_n \approx 125$).⁵ The obtained volume fraction of spherical objects yields the amount of **BTA (*R*)-Cha** present as dimers: 77% of **BTA (*R*)-Cha** is incorporated into stacks which means that the fraction of **BTA (*R*)-Cha** in the stacks is 0.33 (f Cha in stacks^{SANS} = 0.33). The radius (10.4 Å) and number of molecules in the cross-section ($n=0.6$) were extracted from this SANS curve after removing the contribution of dimers. These values are consistent with the co-assembly being isolated stacks of BTA molecules.

[c] In our previous publication, the length determined by SANS for **BTA^{PPh2}** and for the mixture of **BTA^{PPh2}** and **BTA (*S*)-Cha** (Fig. S5 in ref [1])¹ was under evaluated as a result of the interactions between objects at the higher concentrations employed in these analyses.

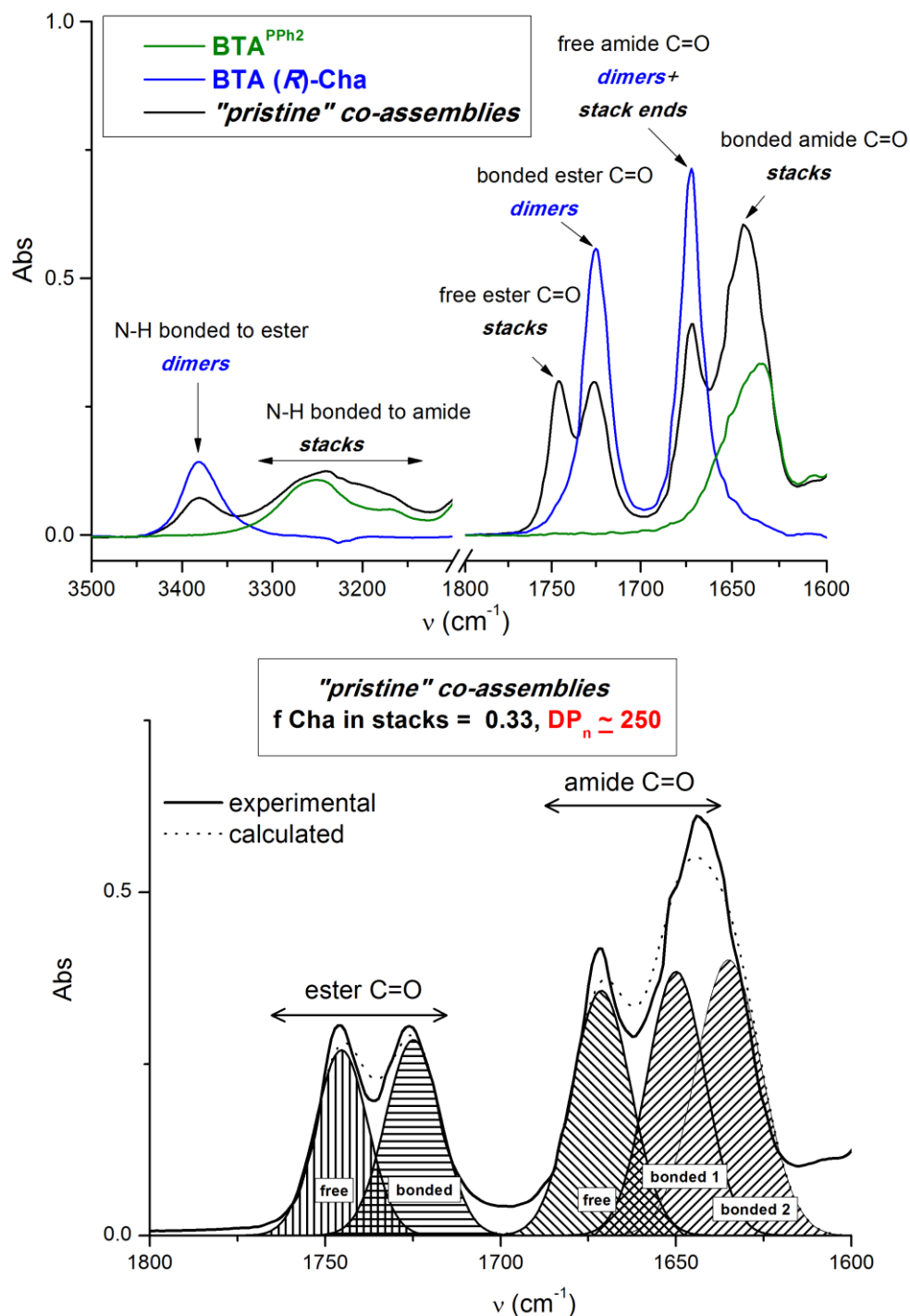


Figure S2 Characterization of the co-assemblies by FT-IR analyses (293 K, C_7D_8). Top: Assignment of the N-H and C=O bands in the homo- and co-assemblies.^{2, 6, 7} Bottom: Deconvoluted FT-IR spectrum of the co-assemblies (C=O region).^{[a],[b],[c]}

[a] Composition (The concentrations are close to those employed in the catalytic experiments.): **BTA^{PPh2}**: [BTA^{PPh2}] = 16.7 mM, **BTA (R)-Cha**: [BTA (R)-Cha] = 18.4 mM, **“pristine” co-assemblies**: [BTA^{PPh2}] = 16.7 mM, [BTA (R)-Cha] = 18.4 mM.

[b] Value obtained after deconvolution: $f \text{ Cha in stacks}^{\text{FT-IR}} = 0.33$. This value is in good agreement with that obtained previously by processing the N-H region of the FT-IR spectrum ($f \text{ Cha in stacks}^{\text{FT-IR}} = 0.35$).¹ The fact that SANS analyses (Fig. S1) give the same value under different conditions is fortuitous.

[c] The concentration of stack ends is too low to be reliably determined so that the indicated DP_n value is deduced from SANS analysis (Fig. S1) by considering that the concentrations are here *ca.* 4 times higher.⁵

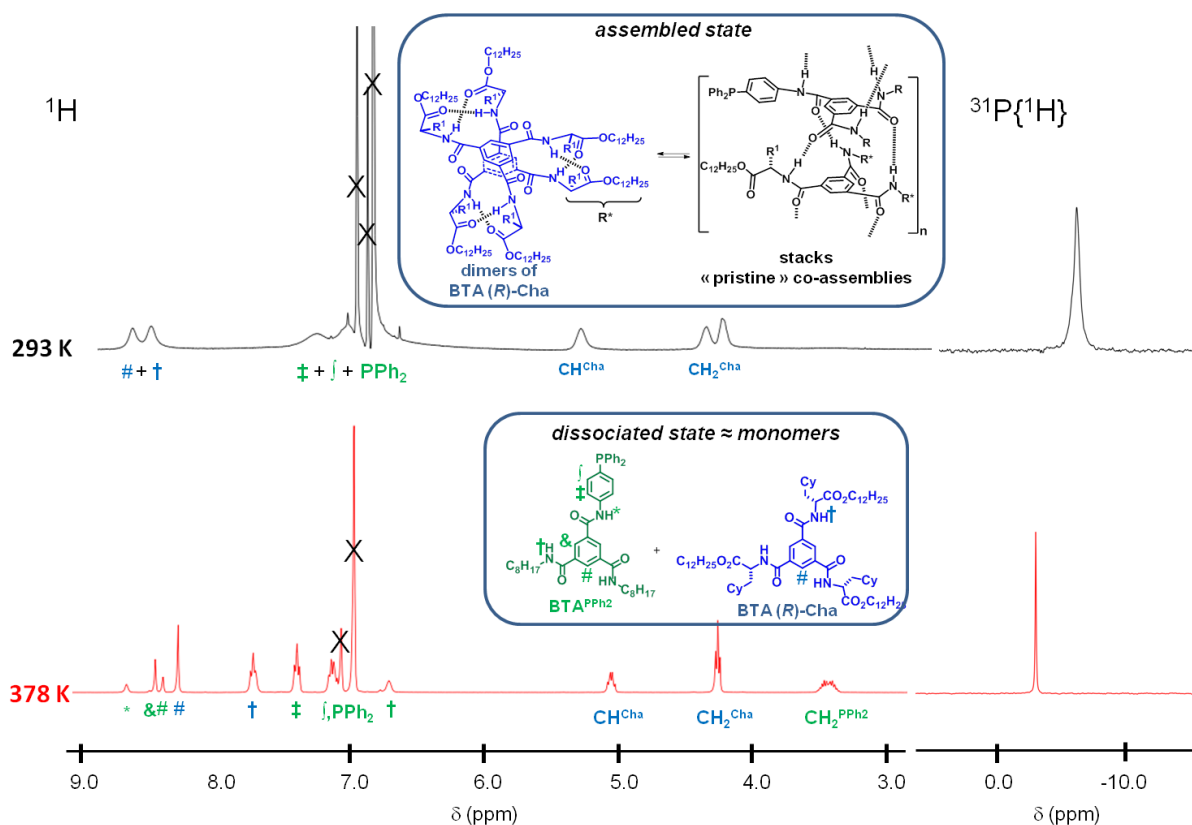


Figure S3 Characterization of the co-assemblies by ^1H and $^{31}\text{P}\{^1\text{H}\}$ NMR analyses. Sample “pristine” co-assemblies at 378 K and 293 K (C_7D_8).^[a] x = residual protons of C_7D_8 .

[a] Interpretation: At 378 K: the fact that the signals are well-defined is consistent with the presence of a dissociated state in which all molecules are monomers (or weakly associated). Assignment of the different protons has been made based on the ^1H NMR analyses of the individual molecules (data not shown). At 293 K: the fact that the signals broaden upon lowering the temperature is indicative of the formation of assemblies.^{2, 8, 9} At this temperature, the observed signals are attributed to $\text{BTA}(\text{R})\text{-Cha}$ and to the aryl rings connected to the phosphorus atoms of $\text{BTA}^{\text{PPh}_2}$ in the co-assemblies; all the others signals are too broad to be detected. We attribute the detected signals of $\text{BTA}(\text{R})\text{-Cha}$ to dimers in equilibrium with the co-assemblies (stacks). The singlet corresponding to the PPh_2 group ($^{31}\text{P}\{^1\text{H}\}$ NMR analyses) also broadens upon formation of the assemblies.

Characterization of the “pristine” co-assemblies coordinated to Cu (Fig. S4).

$^{31}\text{P}\{^1\text{H}\}$ NMR analysis (Fig. S4a) of the **BTA^{PPh₂}-BTA (R)-Cha** mixture in presence of $\text{Cu}(\text{OAc})_2\cdot\text{H}_2\text{O}$ clearly shows two singlets: one (broad) corresponding to Cu coordinated to phosphine ($\delta = -1.5$ ppm) and one corresponding to free phosphine ($\delta = -5.5$ ppm). This indicates that, in the co-assemblies, only a fraction of the phosphine ligands are coordinated to Cu. ^1H NMR spectra of the **BTA^{PPh₂}-BTA (R)-Cha** mixture with and without $\text{Cu}(\text{OAc})_2\cdot\text{H}_2\text{O}$ are similar which shows that the presence of Cu does not disturb much the aggregation. No significant change in the hydrogen-bond network is observed either, upon coordination to Cu (FT-IR, Fig. S4b). SANS analysis reveals that the presence of Cu does not significantly influence the composition and shape of the co-assemblies (see the Table below and Fig. S4c). Co-assemblies with Cu are slightly longer which can be attributed to the fact that the basic character (and thus the hydrogen bond competition) of the PPh₂ group is withdrawn upon coordination. These analyses thus corroborate that the size of the catalytic helices can be roughly estimated by determining the length of the co-assemblies without copper (Figs. S5 to S7).

Comparison of the geometrical features of the co-assemblies with and without Cu as deduced from SANS analyses.^{[a],[b]}

sample	[BTA ^{PPh₂}]	[BTA(R)-Cha]	[Cu(OAc) ₂ ·H ₂ O]	r (Å) ^[b]	n	length(Å)/DP _w ^[b]	f Cha in stacks ^[b]
SANS co-assemblies	3.98 g.L ⁻¹ 5.8 mM	4.39 g.L ⁻¹ 3.7 mM	-	10.4	0.6	870/250	0.33
SANS co-assemblies·Cu	3.99 g.L ⁻¹ 5.77 mM	4.37 g.L ⁻¹ 3.72 mM	0.58 g.L ⁻¹ 2.90 mM	11.4	0.6	>1000/>280	0.34

[a] For comparing the SANS spectra, see Figure 4c. For the fitting procedure, see captions of Figures S1 and S5.

[b] The presence of copper does not modify significantly the structure of the co-assemblies in term of dimensionality and composition. Co-assemblies with Cu are slightly longer which can be attributed to the fact that the basic character of PPh₂ group is withdrawn upon coordination.

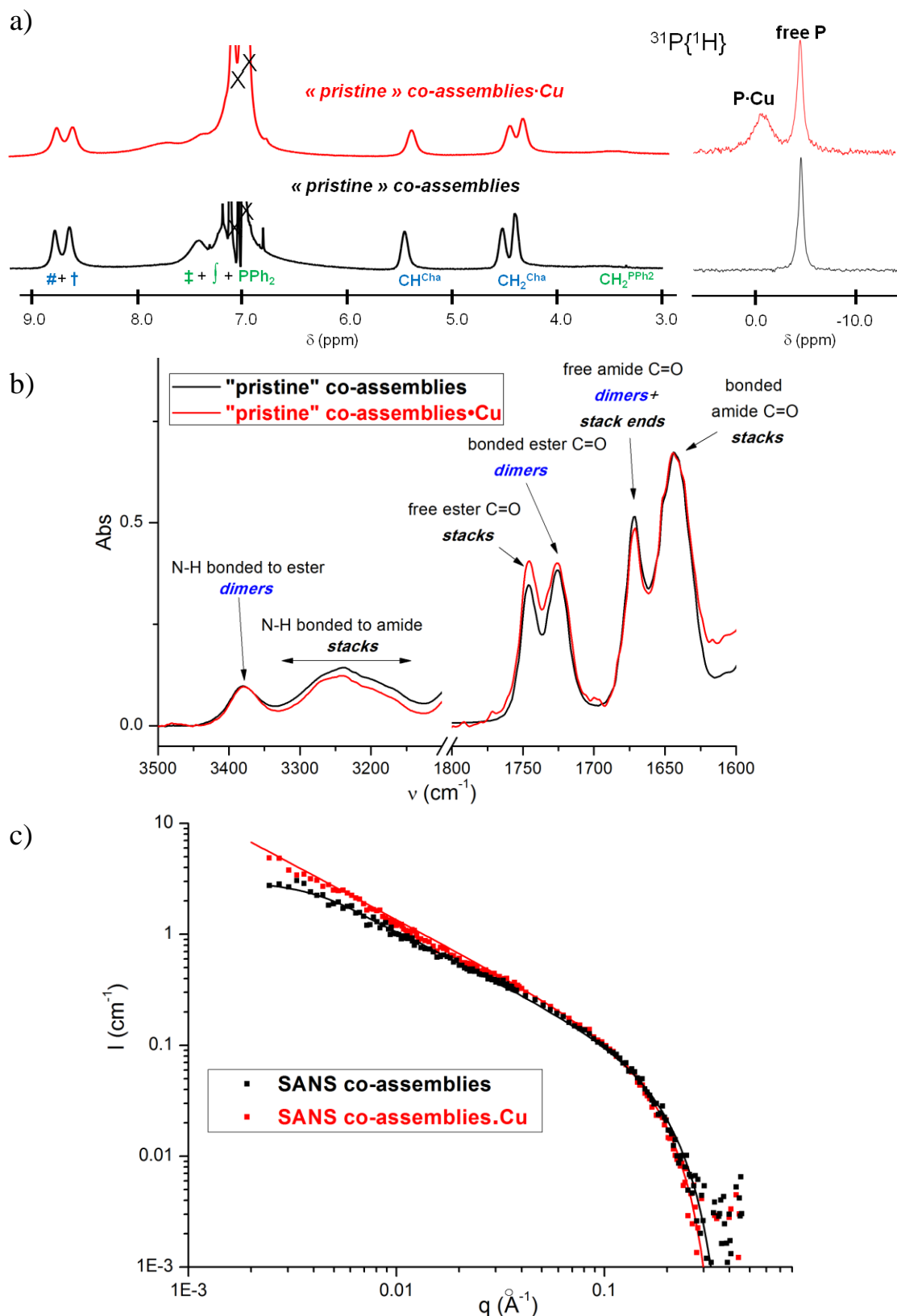


Figure S4 (a) Coordination of copper to the co-assemblies probed by ^1H and $^{31}\text{P}\{^1\text{H}\}$ NMR. Sample "pristine co-assemblies·Cu" analyzed at 293 K and comparison with sample "pristine co-assemblies" (C_7D_8). (b) FT-IR analysis of sample "pristine co-assemblies·Cu" and comparison with sample "pristine co-assemblies" (C_7D_8 , 293 K). (c) SANS analysis of sample "SANS co-assemblies" and comparison with sample "SANS co-assemblies·Cu".

Characterization of the co-assemblies in presence of additives at concentrations *ca.* 4 times lower than those of catalytic experiments (Figs. S5-S6).

The influence of the salts on the nature of the co-assemblies is probed by SANS at concentrations *ca.* 4 times lower than those employed in catalysis in order to avoid interactions between objects (Fig. S5). In that specific conditions, the salts are poorly dissolved (no co-solvents). The co-assemblies are almost fully disassembled (in presence of TPPCl) and partly reassembled (in presence of TPPCl and NaNTf₂). The SANS samples are analyzed by FT-IR and the resulting spectra are deconvoluted (Fig. S6). It confirms that FT-IR analyses allow a valid estimation of the DP_n value of the BTA co-assemblies.

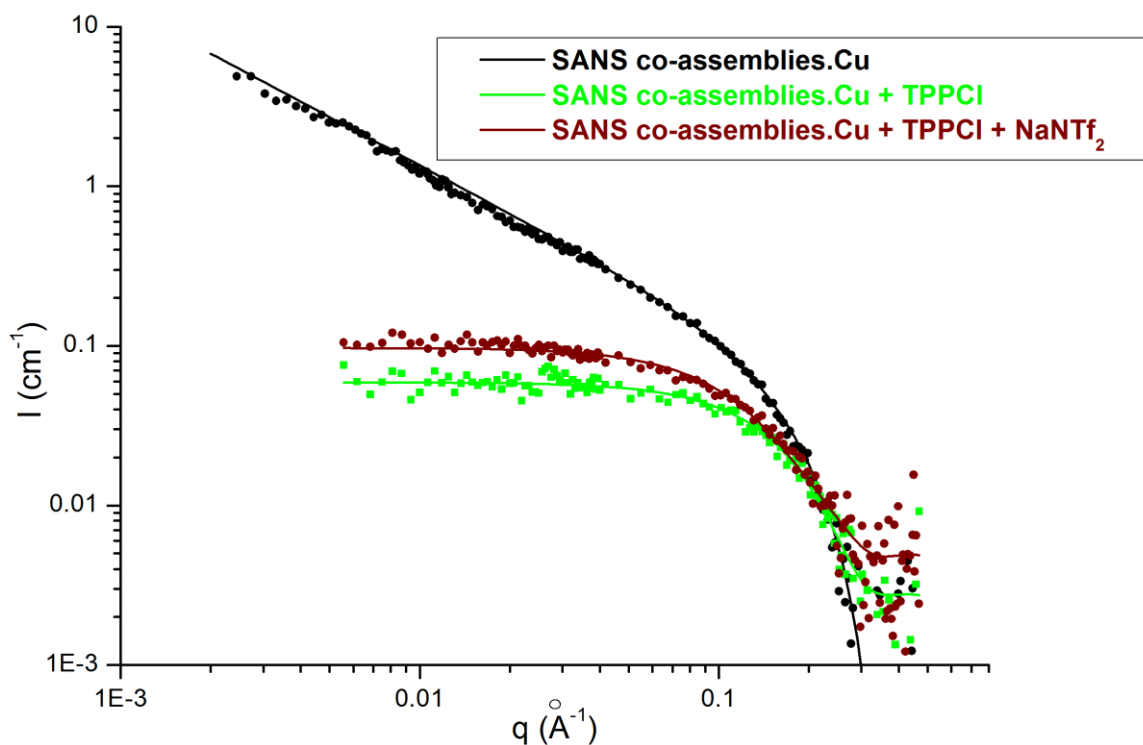


Figure S5 SANS analysis of the samples “SANS co-assemblies·Cu”, “SANS co-assemblies·Cu + TPPCI” and “SANS co-assemblies·Cu + TPPCI + NaNTf₂” (293 K, C₇D₈).^{[a],[b],[c],[d]}

[a] Composition:

sample	[BTA ^{PPH2}]	[BTA(R)-Cha]	[Cu(OAc) ₂ ·H ₂ O]	[TPPCI]	[NaNTf ₂]	r (Å) ^[b]	length(Å)/DP _w ^[b]	DP _n ^[d]
SANS co-assemblies·Cu	4.03 g.L ⁻¹ 5.81 mM	4.42 g.L ⁻¹ 3.76 mM	0.59 g.L ⁻¹ 2.94 mM	-	-	11.4	>1000/>280	
SANS co-assemblies·Cu + TPPCI	3.99 g.L ⁻¹ 5.77 mM	4.37 g.L ⁻¹ 3.72 mM	0.58 g.L ⁻¹ 2.90 mM	2.58 g.L ⁻¹ 6.88 mM	-	-	25/7	5
SANS co-assemblies·Cu + TPPCI + NaNTf₂	4.00 g.L ⁻¹ 5.77 mM	4.38 g.L ⁻¹ 3.72 mM	0.58 g.L ⁻¹ 2.92 mM	2.55 g.L ⁻¹ 6.81 mM	1.72 g.L ⁻¹ 5.66 mM	-	41/11	8
catalytic system (Table S3, run 3) toluene:DCM:acetone 15:1:1	13.8 mM	15.2 mM	6.9 mM	13.8 mM	13.8 mM			

[b] The curves are fitted according to a form factor for rigid rods of infinite length (sample without salt) or finite length (with salt) with a circular cross-section and a uniform scattering length density. The weight-average degrees of polymerization (DP_w) are calculated by dividing the obtained length by the distance between two BTAs in the stacks (≈ 3.5 Å). It gives a length of 25 Å (DP_w ≈ 7) and 41 Å (DP_w ≈ 11) for the sample with TPPCI and the sample with both TPPCI and NaNTf₂, respectively.

[c] Interpretation: The DP_w values are in qualitative agreement with a shortening and lengthening of the assemblies but do not reflect the true length of the BTA assemblies during the catalytic reaction given that the conditions for the SANS and catalytic experiments are very different. Also, the poor solubility of NaNTf₂ in the conditions employed in the SANS analysis (pure C₇D₈) may explain the limited size of the objects formed upon reassembly. The DP_w value of the BTA co-assemblies determined by SANS analyses correlates well with those obtained by deconvolution of the FT-IR spectra (Fig. S6).

[d] Determined by deconvolution of the corresponding FT-IR spectra (Fig. S6).

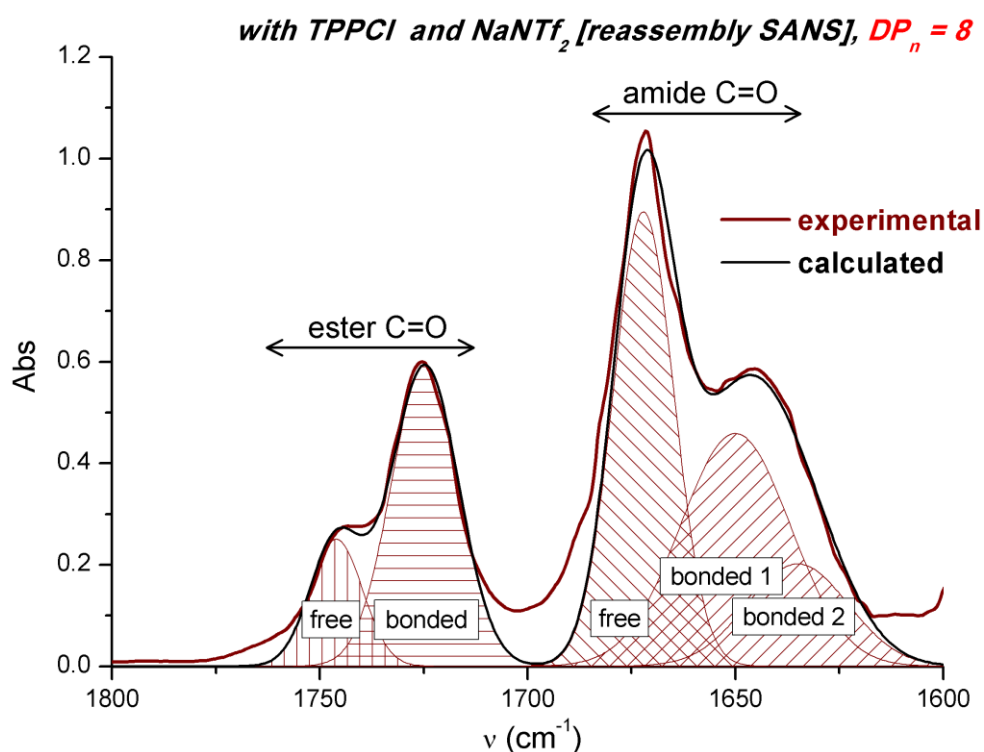
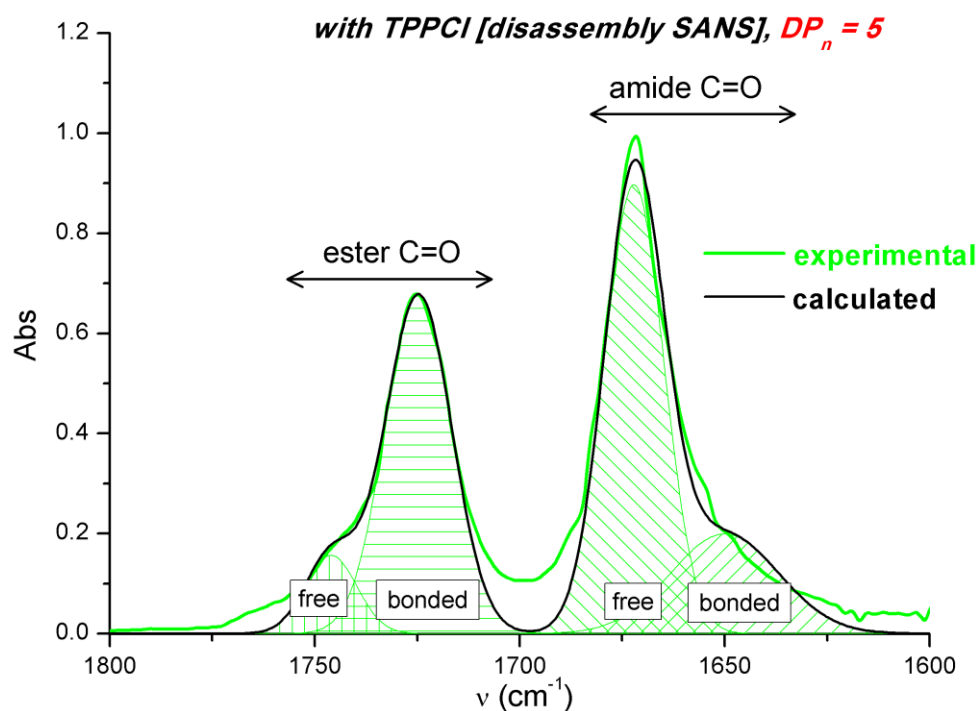


Figure S6 Deconvoluted FT-IR spectra of the solutions analyzed by SANS (Fig. S4). See the precise composition and conditions of the preparation of the samples in Fig. S4.^{[a],[b]}

[a] Values obtained after deconvolution: bonded amide peak 1 ($\nu=1650\text{ cm}^{-1}$, width= 13 cm^{-1}), bonded amide peak 2 ($\nu=1635\text{ cm}^{-1}$, width= 12 cm^{-1} , $\epsilon=35090\text{ L}\cdot\text{mol}^{-1}\cdot\text{cm}^{-1}$), free amide ($\nu=1672\text{ cm}^{-1}$, width= 7 cm^{-1} , $\epsilon=40380\text{ L}\cdot\text{mol}^{-1}\cdot\text{cm}^{-1}$), bonded ester ($\nu=1725\text{ cm}^{-1}$, width= 8 cm^{-1} , $\epsilon=38560\text{ L}\cdot\text{mol}^{-1}\cdot\text{cm}^{-1}$) and free ester ($\nu=1746\text{ cm}^{-1}$, width= 6 cm^{-1}). The obtained DP_n values are indicated in red next to the title.

[b] The fact that the values obtained from processing of the FT-IR spectra are close to that determined by SANS (Fig. S4) confirm that our deconvolution procedure provides a valid estimation of the DP_n values.

Characterization of the co-assemblies in presence of additives at concentrations close to those of catalytic experiments (Figs. 2, S7-S8).

The influence of the salts on the nature of the co-assemblies is probed by FT-IR (Figs. 2a and S7) and NMR (Fig. S8) at concentrations close to those employed in catalysis. FT-IR analyses indicate that the co-assemblies are disassembled in presence of TPPCl and partly re-assembled in presence of both TPPCl and NaNTf₂ (see the changes in the intensities of free amide and bonded amide bands, Fig. 2a). NMR analyses are in agreement with these observations (Fig. S8). Deconvolution of the FT-IR spectra allow the determination of the fraction of **BTA (R)-Cha** in stacks and an estimation of the DP_n values, the latter being in agreement with full disassembly and incomplete reassembly processes (Fig. S7). The incomplete reassembly process is due to presence of acetone-d₆ and CD₂Cl₂ as confirmed by similar FT-IR and ¹H NMR spectra and estimated DP_n values for the samples in presence and absence of TPPCl and NaNTf₂ analyzed in the same solvent mixture (C₇D₈:CD₂Cl₂:acetone-d₆ 15:1).

Composition: **“pristine co-assemblies” (“run 1”)**: [BTA^{PPh₂}] = 16.7 mM, [BTA (R)-Cha] = 18.4 mM, C₇D₈; **“co-assemblies + TPPCl” (“run 2”)**: [BTA^{PPh₂}] = 15.7 mM, [BTA (R)-Cha] = 17.3 mM, [TPPCl] = 15.7 mM, C₇D₈:CD₂Cl₂ 15:1; **“co-assemblies + TPPCl + NaNTf₂” (“run 3”)**: [BTA^{PPh₂}] = 14.7 mM, [BTA (R)-Cha] = 16.2 mM, [TPPCl] = 14.7 mM, [NaNTf₂] = 14.7 mM, C₇D₈:CD₂Cl₂:acetone-d₆ 15:1:1; **“co-assemblies + DCM + acetone” (“run 3 without salts”)**: [BTA^{PPh₂}] = 14.7 mM, [BTA (R)-Cha] = 16.2 mM, C₇D₈:CD₂Cl₂:acetone-d₆ 15:1:1.

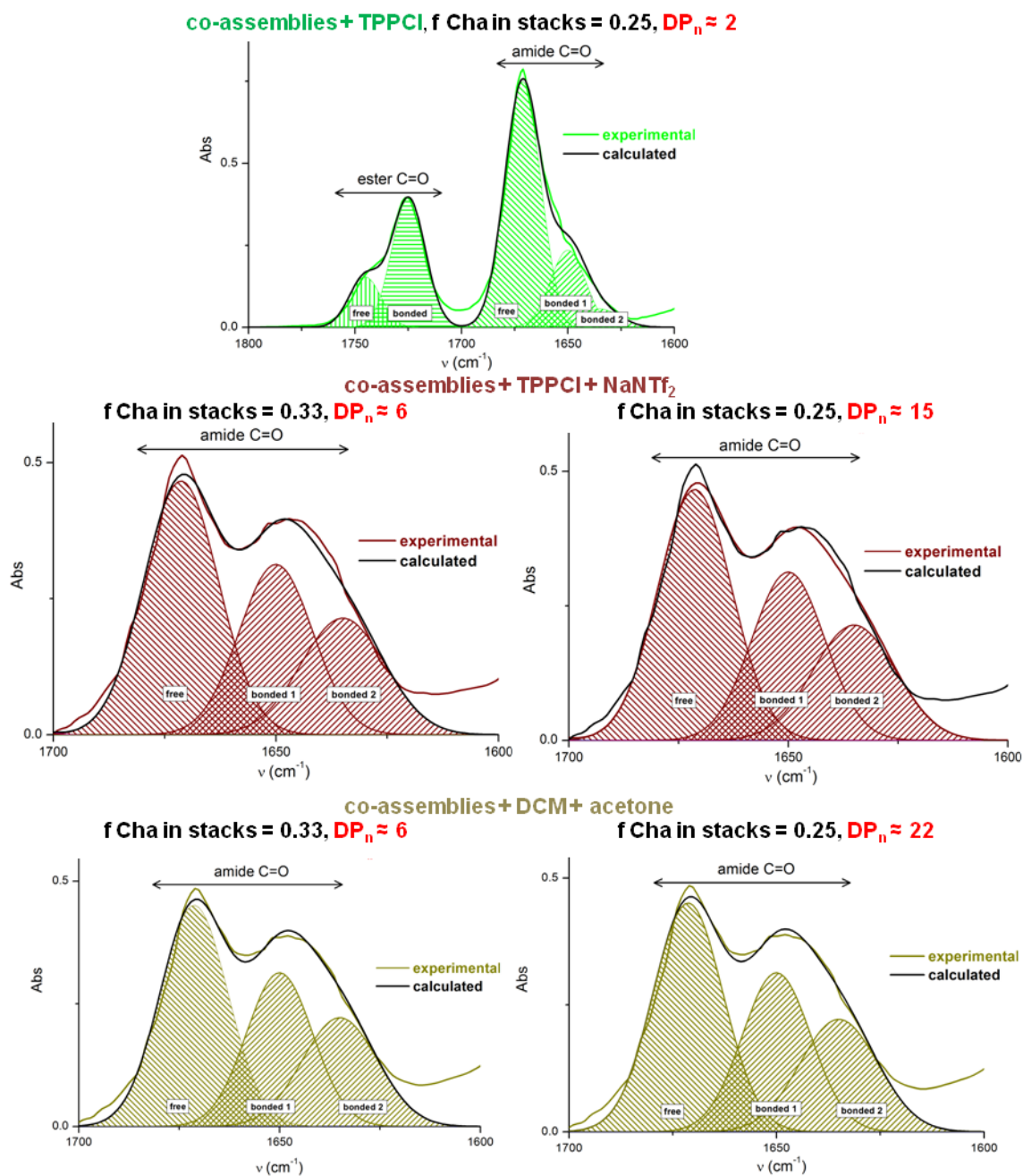


Figure S7 Deconvoluted FT-IR spectrum of the samples “co-assemblies + TPPCI”, “co-assemblies + TPPCI + NaNTf₂” and “co-assemblies + DCM + acetone” (293 K).^{[a],[b]}

[a] For samples “co-assemblies + TPPCI + NaNTf₂” and “co-assemblies + DCM + acetone”, the presence of acetone prevents the deconvolution of the ester C=O bands. A range of DP_n values was determined by assuming two extreme values of f Cha in stacks: 0.25, *i.e.* the value obtained upon full disassembly, and 0.33, *i.e.* the value in the pristine co-assemblies.

[b] *Values obtained after deconvolution:* bonded amide peak 1 ($\nu=1650\text{ cm}^{-1}$, width=8 cm^{-1}), bonded amide peak 2 ($\nu=1635\text{ cm}^{-1}$, width=10 cm^{-1} , $\epsilon=31750\text{ L}\cdot\text{mol}^{-1}\cdot\text{cm}^{-1}$), free amide ($\nu=1671\text{ cm}^{-1}$, width=8 cm^{-1} , $\epsilon=34180\text{ L}\cdot\text{mol}^{-1}\cdot\text{cm}^{-1}$), bonded ester ($\nu=1725\text{ cm}^{-1}$, width=8 cm^{-1} , $\epsilon=28950\text{ L}\cdot\text{mol}^{-1}\cdot\text{cm}^{-1}$) and free ester ($\nu=1745\text{ cm}^{-1}$, width=7 cm^{-1}). These values are in agreement with those obtained by deconvoluting the FT-IR corresponding to the samples analyzed by SANS (Fig. S5).

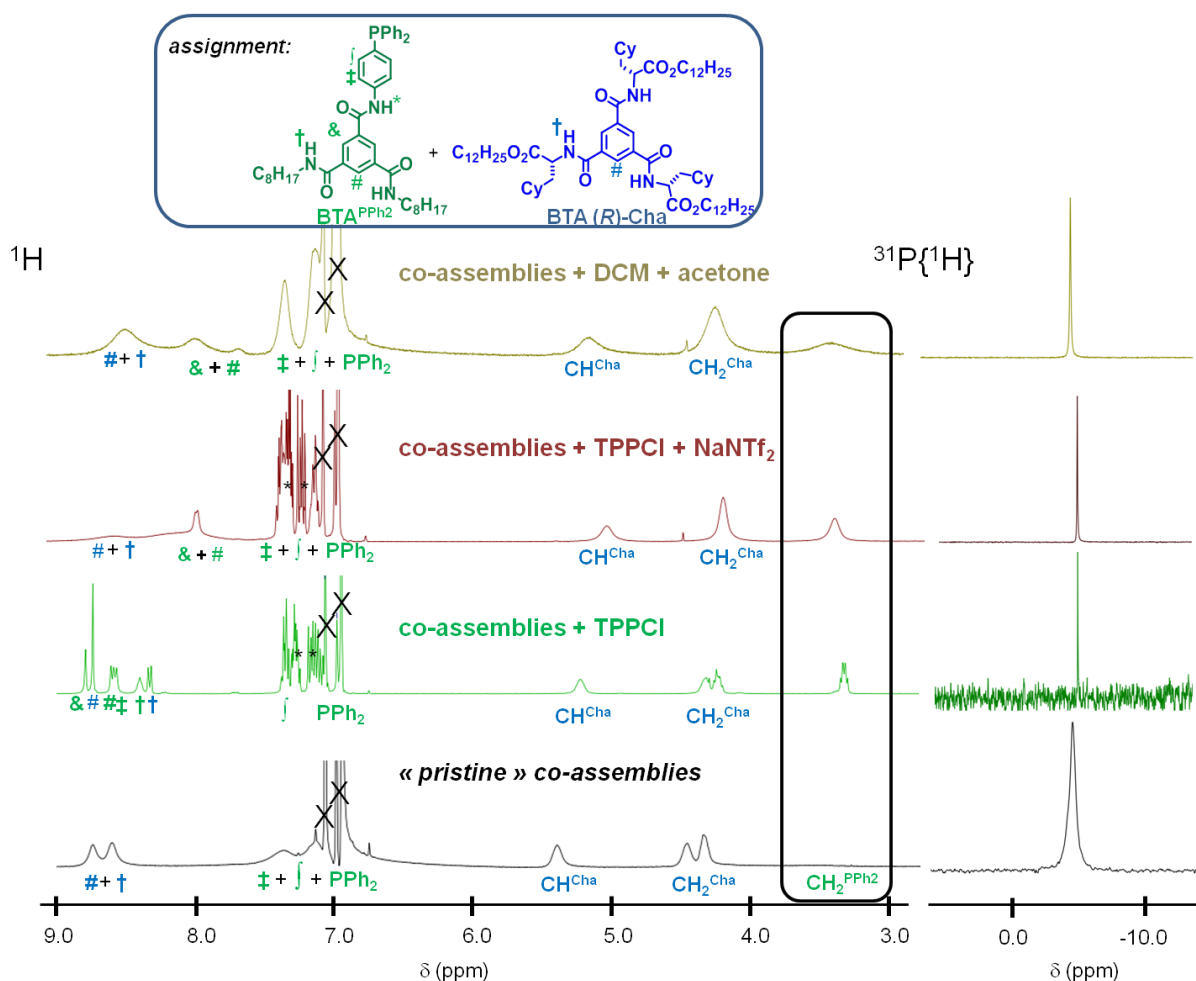


Figure S8 ^1H and $^{31}\text{P}\{^1\text{H}\}$ NMR analyses of the samples “pristine co-assemblies”, “co-assemblies + TPPCI”, “co-assemblies + TPPCI + NaNTf₂”, and “co-assemblies + DCM + acetone” (293 K).^[a] x = residual protons of C₇D₈, * = proton signals of TPPCI. For the sample “co-assemblies + TPPCI” the proton signal labelled as * is downfield shifted to ≈ 11 ppm. The ^{31}P signal of TPPCI ($\delta \approx 23$ ppm) is not shown.

[a] Interpretation: ^1H NMR analyses of the samples “co-assemblies + TPPCI”, “co-assemblies + TPPCI + NaNTf₂” and “co-assemblies + DCM + acetone” can be interpreted in the same way as that of sample “pristine co-assemblies” (see caption [a] in Fig. S3) with the exception that additional signals corresponding to $\text{BTA}^{\text{PPh}_2}$ can be detected as a result of the decreased length of the co-assemblies in these samples. In fact, the width of proton signal $\text{CH}_2^{\text{PPh}_2}$ (surrounded in black) and of the phosphorus signal of the PPh₂ group reflects the degree of polymerization which increases in the following order: “co-assemblies + TPPCI” < “co-assemblies + TPPCI + NaNTf₂” \approx “co-assemblies + DCM + acetone” < “pristine co-assemblies”.

Summary of the structural data and correlation between length and selectivity (Table S2).

Table S2 Structural data and relation between the selectivity and the length for the different samples investigated in this study.

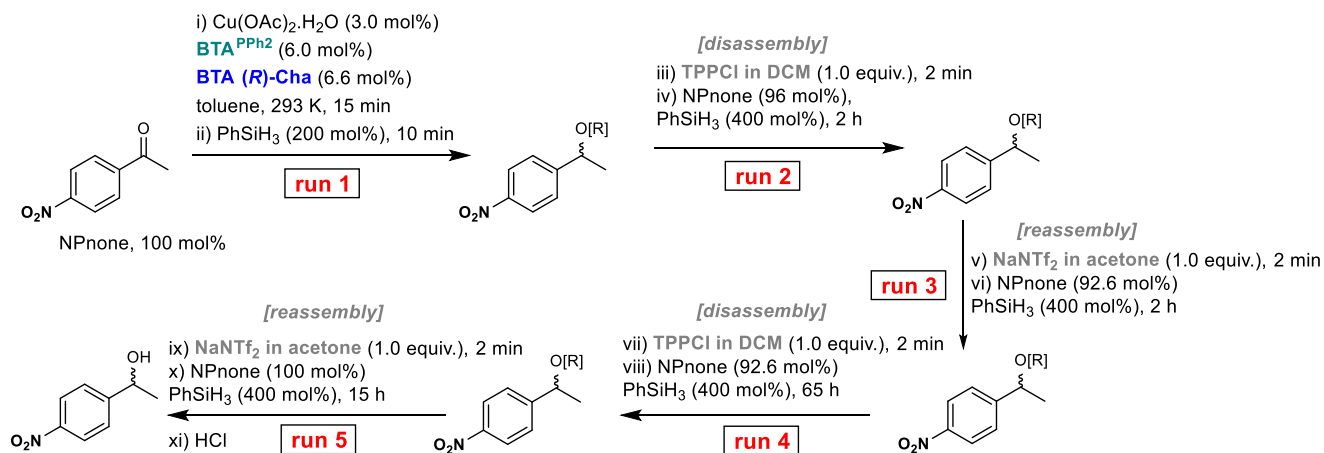
sample	“run”	DP _n ^[a]	f Cha in stacks ^{FT-IR[a]}	<i>e.e.</i> (%)
“pristine” co-assemblies	run 1	≈ 250 ^[b]	0.33	51
co-assemblies + TPPCI	run 2	≈ 2	0.25	0-6
co-assemblies + TPPCI + NaNTf ₂	run 3	6-15	0.25-0.33	43
co-assemblies + DCM + acetone	run 3 without salts	6-22	0.25-0.33	37

[a] DP_n and f Cha in stacks values were determined by FT-IR analyses unless otherwise stated.

[b] Deduced from SANS analysis (Fig. S1).

Reversible switch of the selectivity (Table S3).

Table S3 Copper-catalysed hydrosilylation of 1-(4-nitrophenyl)ethanone with successive additions of substrate, salt (TPPCL or NaNTf₂) and PhSiH₃.^[a]



run	substrate (subs ⁰ n)	cumulated substrate (subs n) ^[b]	cumulated conversion (cconv n) ±0.5%	cumulated enantioselectivity (c e.e. n) ±0.5%	conversion for the run (conv n) ±0.5% ^[c]	enantioselectivity for the run (e.e. n) ^[d]
1	100	100	99	52	99	52±0.5%
2	96	97	93	31	86	6±1.0%
3	92.6	106.3	96	35	89	43±1.5%
4	92.6	104.1	87	29	53	0±5%
5	100	149.6	95	29	84	29±5%

[a] Reaction conditions: 1-(4-nitrophenyl)ethanone (subs⁰ 1=100 mol%^{run1}, subs⁰ 2 = 96 mol%^{run2}, subs⁰ 3 = 92.6 mol%^{run3}, subs⁰ 4 = 92.6 mol%^{run4}, subs⁰ 5 = 100 mol%^{run5} = 481.2 mol% in total), Cu(OAc)₂·H₂O (3.0 mol%), **BTA**^{PPh₂} (6.0 mol%), **BTA (R)-Cha** (6.6 mol%), PhSiH₃ (100 mol% for run 1 and then 400 mol% for run 2, run 3, run 4 and run 5 = 1700 mol% in total), TPPCL in 40 μL of DCM (1.0 equiv. relatively to **BTA**^{PPh₂} for run 2 and 4), NaNTf₂ in acetone (1.0 equiv. relatively to **BTA**^{PPh₂} for run 3 and 5), toluene (600 μL), 293 K. Conversion (cconv n) and e.e. (c e.e. n) for each run were determined by GC analyses of the aliquots (see pages S-20 to S-22). The conversion and enantioselectivity for each run have been calculated as indicated below.

[b] $\text{subs } n = \text{subs}_0 n + [(1 - \text{cconv } (n - 1)) \times \sum_{i=1}^{n-1} \text{subs}_0 i]$. The amount of substrate is normalized to 100 for 27 mg of 1-(4-nitrophenyl)ethanone (100 mol%).

$$[\text{c}] \quad \text{conv } n = \frac{\text{cconv } n \times \sum_{i=1}^n \text{subs}_0 i - \sum_{i=1}^{n-1} \text{conv } i \times \text{subs } i}{\text{subs } n}$$

[d]

$$e.e. n = \frac{(c.e.e. n \times \sum_{i=1}^n (\text{subs } i \times \text{conv } i)) - \sum_{i=1}^{n-1} (e.e. i \times \text{subs } i \times \text{conv } i)}{\text{conv } n \times \text{subs } n}$$

Catalytic experiments.

In all catalytic experiments a *pre-catalytic mixture* composed of the ligand, the enantiopure co-monomer, the copper salt and the substrate was prepared as follows: a tube was loaded with $\text{Cu}(\text{OAc})_2 \cdot \text{H}_2\text{O}$ (1.0 mg, 3.0 mol%) and $\text{BTA}^{\text{PPh}_2}$ (6.9 mg, 6.0 mol%) in dry THF (500 μL) and the mixture was stirred for 30 minutes. The solvent was removed under vacuum and the tube was further put under vacuum (1.10^{-3} mbar) for 1 hour. Then 1-(4-nitrophenyl)ethanone (28.0 mg, 0.17 mmol, 100 mol%) was added before flushing the tube with argon for 10 seconds. **BTA (R)-Cha** (12.9 mg, 6.6 mol%) in 100 μL of dry toluene was added to the tube as well as 500 μL dry toluene. The mixture was stirred for 15 min at room temperature.

Influence of the amount of TPPCI on the hydrosilylation of 1-(4-nitrophenyl)ethanone (Fig. 1, Table S1): TPPCI (0.3-1.0 equiv. relatively to $\text{BTA}^{\text{PPh}_2}$) was dissolved in dichloromethane (40 μL), added to the pre-catalytic mixture and the mixture was stirred for 20 seconds. Then, PhSiH_3 (42.0 μL , 0.34 mmol, 200 mol%) was added and the reaction mixture was stirred for 12 hours before being hydrolyzed with aqueous HCl and analyzed by chiral GC.

Hydrosilylation of 1-(4-nitrophenyl)ethanone with sequential additions of salt, substrate and PhSiH_3 (Fig. 3, Table S3): A tube was loaded with $\text{Cu}(\text{OAc})_2 \cdot \text{H}_2\text{O}$ (1.0 mg, 3.0 mol%) and $\text{BTA}^{\text{PPh}_2}$ (6.9 mg, 6.0 mol%) in dry THF (500 μL) and the mixture was stirred for 30 minutes. The solvent was removed under vacuum and the tube was further put under vacuum (1.10^{-3} mbar) for 1 hour. Then 1-(4-nitrophenyl)ethanone (27.0 mg, 0.16 mmol, 100 mol%) was added before flushing the tube with argon for 10 seconds. **BTA (R)-Cha** (12.9 mg, 6.6 mol%) in 100 μL of dry toluene was added to the tube as well as 500 μL dry toluene. The mixture was stirred for 15 min at room temperature. PhSiH_3 (42.0 μL , 0.34 mmol, 200 mol%) was added and the mixture was stirred for 10 minutes. An aliquot (40 μL) was taken up, hydrolyzed with aqueous HCl and analyzed by chiral GC (*run 1*). **TPPCI** (3.7 mg, 1.0 equiv. relatively to $\text{BTA}^{\text{PPh}_2}$) in dichloromethane (40 μL) was added and the solution was stirred for 2 minutes before addition of 1-(4-nitrophenyl)ethanone (26.4 mg, 0.16 mmol, 96 mol%) and PhSiH_3 (84.0 μL , 0.68 mmol, 400 mol%). The mixture was stirred for 2 h and an aliquot of 40 μL was taken up, hydrolyzed with aqueous HCl and analyzed by chiral GC (*run 2*). **NaNTf₂** (3.0 mg, 1.0 equiv. relatively to $\text{BTA}^{\text{PPh}_2}$) in acetone (40 μL) was added and the mixture was stirred for 2 minutes before addition of 1-(4-nitrophenyl)ethanone (25.0 mg, 0.15 mmol, 92.6 mol%) and PhSiH_3 (84.0 μL , 0.68 mmol, 400 mol%). The mixture was stirred for 2 hours and an aliquot of 40 μL was taken up, hydrolyzed with aqueous HCl and analyzed by chiral GC (*run 3*). **TPPCI** (3.7 mg, 1.0 equiv. relatively to $\text{BTA}^{\text{PPh}_2}$) in dichloromethane (40 μL) was added and the solution was stirred for 2 minutes before addition of 1-(4-nitrophenyl)ethanone (25.0 mg, 0.15 mmol, 92.6 mol%) and PhSiH_3 (84.0 μL , 0.68 mmol, 400 mol%). The mixture was stirred for 65 hours and an aliquot of 40 μL was taken up, hydrolyzed with aqueous HCl and analyzed by chiral GC (*run 4*). **NaNTf₂** (3.0 mg, 1.0 equiv. relatively to $\text{BTA}^{\text{PPh}_2}$) in acetone (40 μL) was added and the mixture was stirred for 2 minutes before addition of 1-(4-nitrophenyl)ethanone (27.0 mg, 0.16 mmol, 100 mol%) and PhSiH_3 (84.0 μL , 0.68 mmol, 400 mol%). The mixture was stirred for 15 hours, hydrolyzed with aqueous HCl and analyzed by chiral GC (*run 5*).

GC analyses from the aliquots of the different run.

Table S3, run 1:

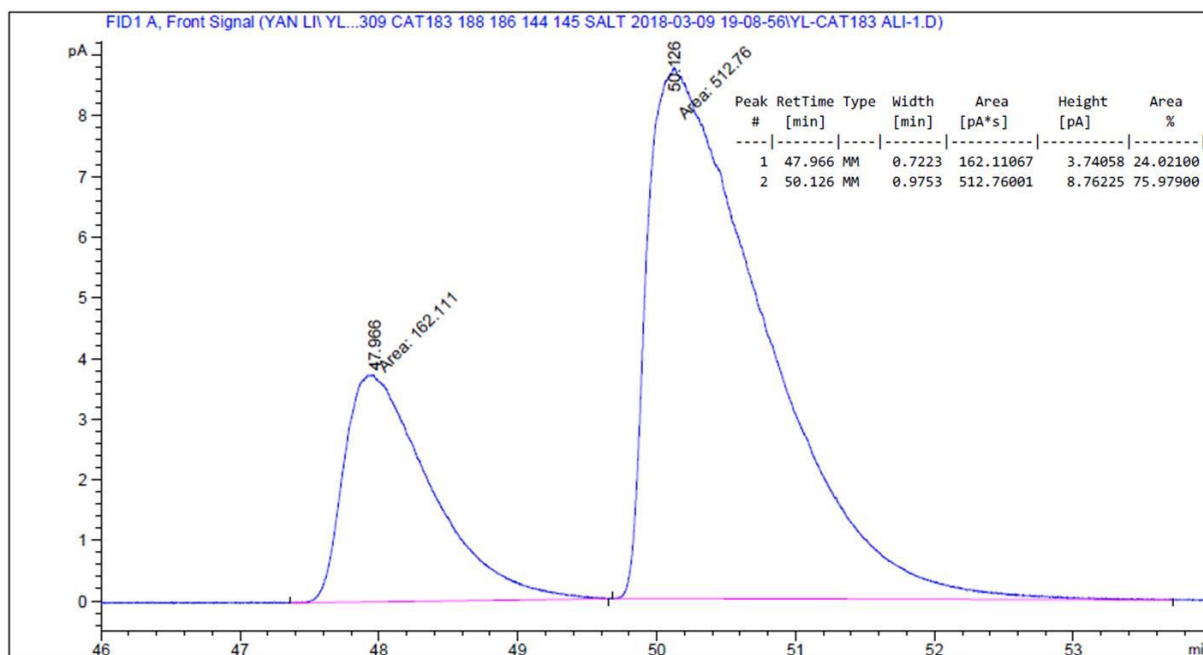


Table S3, run 2:

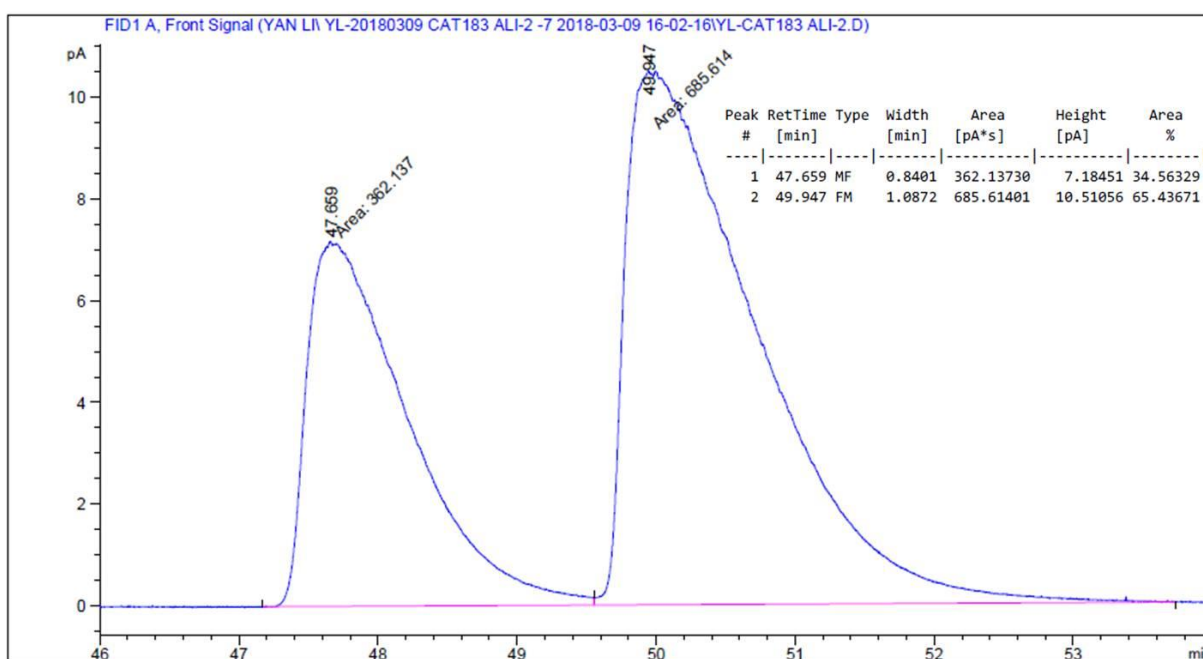


Table S3, run 3:

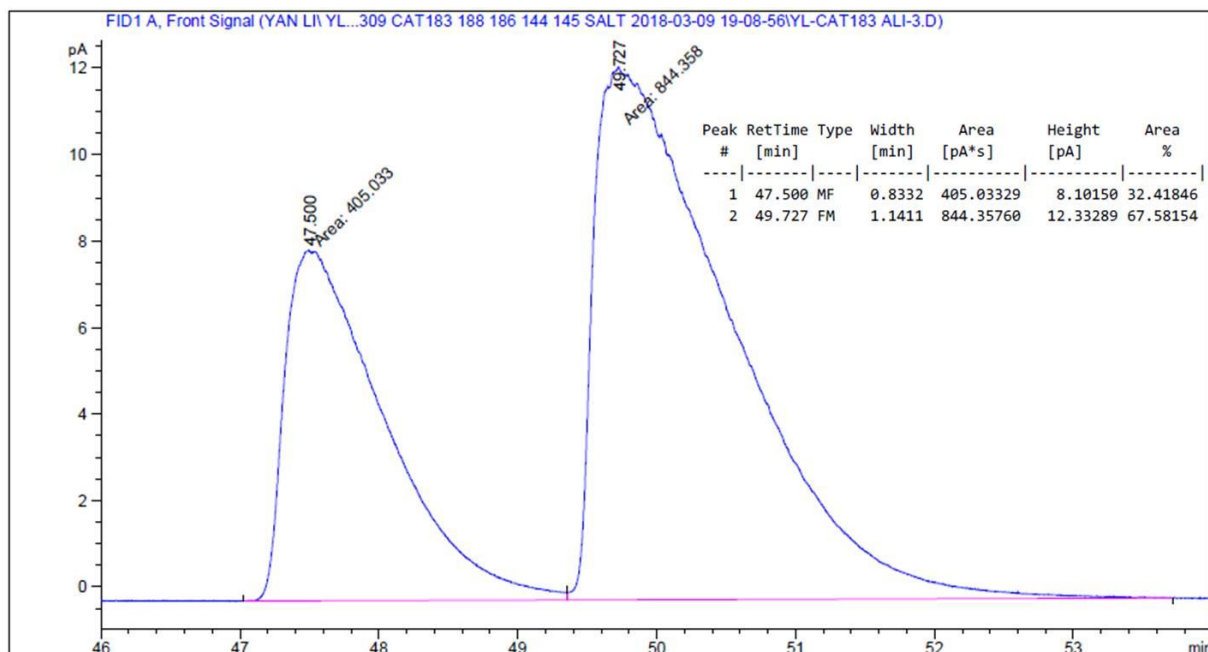


Table S3, run 4:

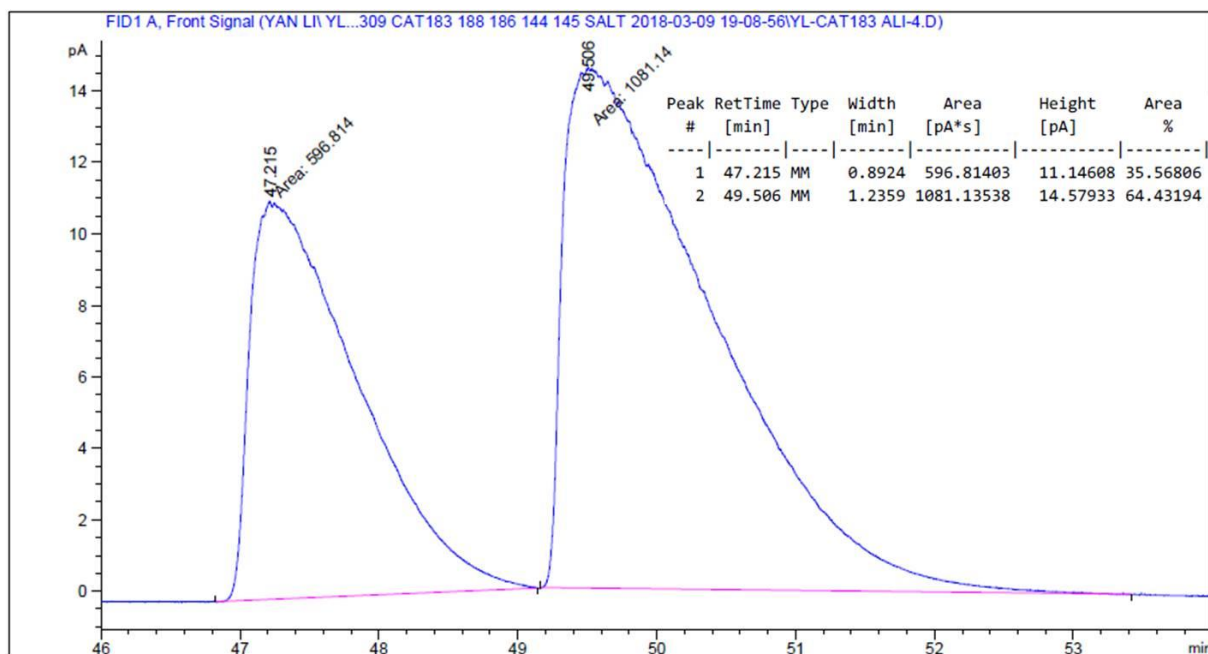
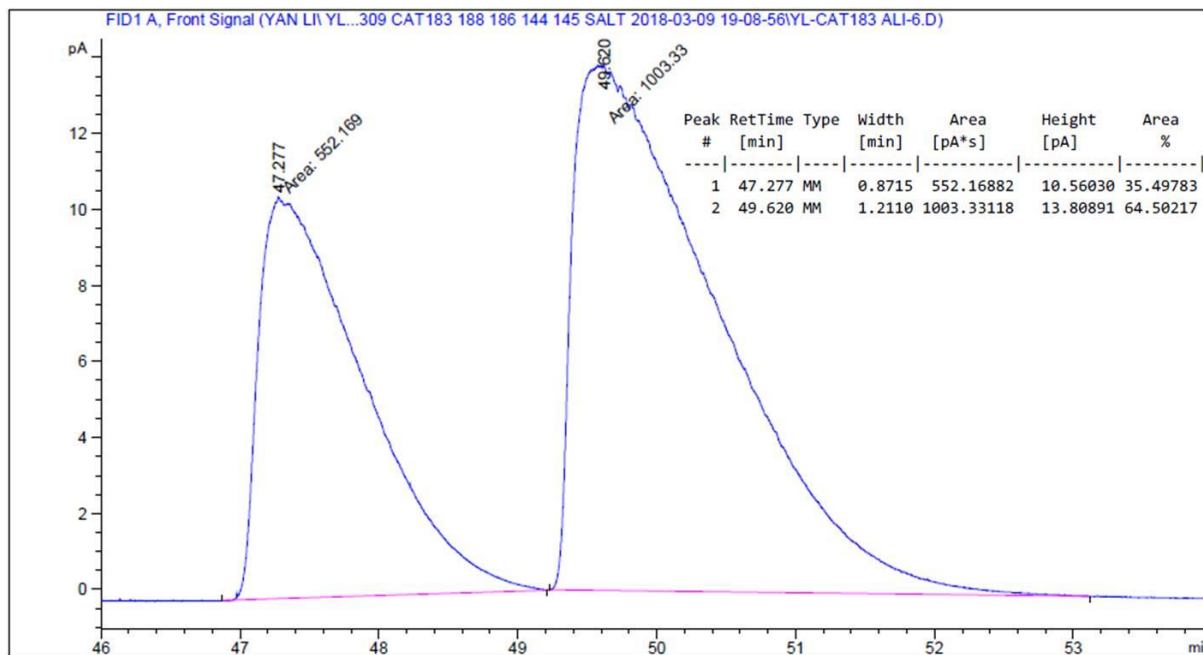


Table S3, run 5:



References.

1. J. M. Zimbron, X. Caumes, Y. Li, C. M. Thomas, M. Raynal and L. Bouteiller, *Angew. Chem. Int. Ed.*, 2017, **56**, 14016-14019.
2. A. Desmarchelier, B. Giordano Alvarenga, X. Caumes, L. Dubreucq, C. Troufflard, M. Tessier, N. Vanthuyne, J. Idé, T. Maistriaux, D. Beljonne, P. Brocorens, R. Lazzaroni, M. Raynal and L. Bouteiller, *Soft Matter*, 2016, **12**, 7824-7838.
3. F. Lortie, S. Boileau, L. Bouteiller, C. Chassenieux, B. Deme, G. Ducouret, M. Jalabert, F. Laupretre and P. Terech, *Langmuir*, 2002, **18**, 7218-7222.
4. G. Uray, W. Stampfer and W. M. F. Fabian, *J. Chromatogr. A*, 2003, **992**, 151-157.
5. T. F. A. De Greef, M. M. J. Smulders, M. Wolffs, A. P. H. J. Schenning, R. P. Sijbesma and E. W. Meijer, *Chem. Rev.*, 2009, **109**, 5687-5754.
6. A. Desmarchelier, M. Raynal, P. Brocorens, N. Vanthuyne and L. Bouteiller, *Chem. Commun.*, 2015, **51**, 7397-7400.
7. X. Caumes, A. Baldi, G. Gontard, P. Brocorens, R. Lazzaroni, N. Vanthuyne, C. Troufflard, M. Raynal and L. Bouteiller, *Chem. Commun.*, 2016, **52**, 13369-13372.
8. M. Wegner, D. Dudenko, D. Sebastiani, A. R. A. Palmans, T. F. A. de Greef, R. Graf and H. W. Spiess, *Chem. Sci.*, 2011, **2**, 2040-2049.
9. R. van Hameren, A. M. van Buul, D. Visser, R. K. Heenan, S. M. King, A. E. Rowan, R. J. M. Nolte, W. Pyckhout-Hintzen, J. A. A. W. Elemans and M. C. Feiters, *Soft Matter*, 2014, **10**, 9688-9694.